Morpho Butterfly-Inspired Nanostructures

Haider Butt, Ali K. Yetisen, Denika Mistry, Safyan Akram Khan, Mohammed Umair Hassan, and Seok Hyun Yun*

The wing scales of *Morpho* butterflies contain 3D nanostructures that produce blue iridescent colors. Incident light is diffracted from multilayered nanostructures to create interference effects and diffract narrow-band light. The intensity of the diffracted light remains high over a wide range of viewing angles. Structural coloration originating from the scales of *Morpho* wing nanostructures has been studied to analyze its optical properties and to produce scalable replicas. This review discusses computational and experimental methods to replicate these nanoarchitectures. Analytical and numerical methods utilized include multilayer models, the finite element method, and rigorous coupled-wave analysis, which enable the optimization of nanofabrication techniques involving biotemplating, chemical vapour deposition, electron beam lithography, and laser patterning to mimic the wing scale nanostructure. Dynamic tunability of the morphology, refractive index, and chemical composition of the *Morpho* wing scales allows the realization of a numerous applications.

1. Nanoarchitecture of *Morpho* Wing Scales

Tropical *Morpho* butterflies are known for their iridescence.[1] Extensive research has been dedicated to analyzing the nanoscale architecture of *Morpho* butterfly wings to understand their brilliant blue or white–purple iridescence (see **Figure 1**a).[2–5] Although many hypotheses have been proposed about the nanostructure of the *Morpho* butterfly wing scales, the first electron microscope study of the *Morpho cypris* was carried out by Anderson and Richards in the 1940s.[6,7] Further electron microscope studies led to the classification of the morphological features and the discovery of blue iridescence based on structural color.

The bright blue color irradiated from the *Morpho* butterfly is a combination of diffraction based on multilayer interference and pigmentation (in certain species).[6,10] Under different incident or viewing angles, the color of the *Morpho* butterfly wing slightly changes, suggesting that the blue color does not solely arise from pigmentation, but a nanostructure. *Morpho* species have 'ground' and 'glass' scales.[9,11] The ground scales are the basis of the bright blue color, and lie on the dorsal surface of the wing, where the majority of the interference occurs (Figure 1b).[9] However, the glass scales are highly transparent and situated above the ground scales, acting as an optical diffuser and resulting in a glossy finish to the surface of the wing, while exhibiting relatively low iridescence (Figure 1c). The variation in the nanoarchitecture of scales in different *Morpho* species affects the appearance of the blue intensity displayed.

The scales of a *Morpho* butterfly are composed of periodic ridges made of cuticle, which lie parallel to the edge of the scale and to each other (Figure 1d). The gap separating the ridges is less than 1 µm, and one scale may feature hundreds of these ridges.[12] A single ridge consists of a stack of nanoscale multilayered thin films called lamellae (Figure 1e). Hence, these types of scale were categorized as "ridge lamella". This elaborate structure is the foundation of the bright blue iridescence of *Morpho* butterflies.[13] The origin of the blue color is the multilayer interference caused by the stack of lamellae (**Figure 2**a).[14,15] The blue *Morpho* scale is wavelength selective, since it only scatters the blue region of light from its Christmas tree-resembling structure.[12] This is due to the vertical spacing between lamellae, which is ≈200–300 nm, and approximately equal to half the wavelength of the color that is irradiated from the wing surface.

Each ridge consists of alternating cuticle and air layers, which form the lamellar structure.[6] However, the cuticle layers are randomly distributed over the scale, where the ridges have irregular height differences, and these ridges run parallel to the scale surface.[17,18] This is responsible for the second

Dr. H. Butt, D. Mistry
Nanotechnology Laboratory
School of Engineering
University of Birmingham
Birmingham B15 2TT, UK
E-mail: h.butt@bham.ac.uk

Dr. A. K. Yetisen, Prof. S. H. Yun
Harvard Medical School and Wellman Center for Photomedicine
Massachusetts General Hospital
65 Landsdowne Street, Cambridge, Massachusetts 02139, USA

Dr. A. K. Yetisen, Prof. S. H. Yun
Harvard-MIT Division of Health Sciences and Technology
Massachusetts Institute of Technology
Cambridge, Massachusetts 02139, USA

Dr. S. A. Khan
Center of Excellence in Nanotechnology
King Fahd University of Petroleum & Minerals
Dhahran, Saudi Arabia

Dr. M. U. Hassan
Department of Physics
COMSATS Institute of Information Technology
Islamabad, Pakistan

DOI: 10.1002/adom.201500658

optical phenomenon. The narrow width of the ridges diffracts light, but interference among neighboring ridges is canceled out by the irregularities in height differences, since the light diffracted in these regions superimposes with the interference from the multilayer stacks, resulting in wide-angle diffraction (Figure 2b).[6,19] Additionally, the multilayer is almost ideal since it features two media with a large difference in refractive indices, producing enhanced diffraction effects (Figure 2c).[6]

Some *Morpho* species have pigments underneath their scales. By analyzing diffraction, transmission, and absorption properties, the role of these pigments was studied.[5,6] For example, the *Morpho sulkowskyi* and the *Morpho didius* have identical structures; however, they irradiate different colors. The *Morpho sulkowskyi* features a pearly white wing, whereas the *Morpho didius* has a strong blue color. Although the *Morpho sulkowskyi* has high reflectivity, the strong presence of pigment in the *Morpho didius* absorbs complementary colors, which enhances the contrast of the blue despite its low reflectivity (Figure 2d). The diffraction of colors from *Morpho* butterflies are angle dependent.[16] Figure 2e shows angle-resolved measurements of the back-scattered light from *Morpho rhetenor*, showing the angular dependence of the diffracted light.

Haider Butt is a lecturer (assistant professor) in the School of Engineering, University of Birmingham, UK. Previously, he was a Henslow Research Fellow at the University of Cambridge, UK, where he received his PhD in 2012. His research focusses on photonic devices based on nanostructures like carbon nanotubes, graphene, and plasmonic nanostructures. He has secured several prestigious research awards and has poineered the research on carbon nanotubes based holograms and holographic nanofabrication.

Ali K. Yetisen researches nanotechnology, photonics, biomatercials, government policy, entrepreneurship, and arts. He also lectures at Harvard-MIT Division of Health Sciences and Technology. He holds a PhD in Chemical Engineering and Biotechnology from the University of Cambridge, where he also taught at Judge Business School. He has served as a policy advisor for the British Cabinet Office.

Seok-Hyun (Andy) Yun received his PhD in physics from the Korea Advanced Institute of Science and Technology in 1997. His thesis research led to a startup company in Silicon Valley, where he managed the engineering to produce fiber-optic devices for telecommunications. Currently, he is the Director of the Harvard-MIT Summer Institute for Biomedical Optics. His research areas include optical imaging, photomedicine, biomaterials photonics, and biological lasers.

2. Computational Analyses

Simulations are a low-cost solution to analyze the operation of photonic structures, and offer a range of optimization options to improve performance. Many numerical electromagnetic and optical approaches have been used to analyze the phenomenon of light scattering from butterfly scale nanostructures. Before numerical methods, most approaches were analytical, limiting research to basic geometries. For example, the transfer matrix method had been utilized to model a simplified structure consisting of thin films.[5] Another approach included the lamellar grating theory, where the structure is an x-invariant and each grating layer is y-periodic featuring two regions with differing refractive indices.[20]

The finite difference time domain (FDTD) method has become a practical approach for solving electromagnetic and optical problems. It has the capability to model 3D structures to analyze light interactions within original and fabricated *Morpho* nanostructures; however, some simulations favor analyses in 2D form. The earliest FDTD simulations of *Morpho* structures allowed the classification of their practices as nonstandard finite difference time domain methods (NS-FDTD).[4,21] The algorithm used in NS-FDTD is slightly different than for typical FDTD methods, and a steady state can be reached with fewer iterations. The optical properties of a *Morpho*-inspired computer-generated structure (*Morpho didius*) were investigated to analyze the reflectance spectra.[4,21] Standard FDTD was also utilized for 3D analyses of light scattering by a *Morpho rhetanor* ridge.[22] Recently, the standard form was adopted to analyze the reflectance spectra of an idealized 2D model, and the effect of different parameters on diffraction characteristics.[23]

A different approach to simulate *Morpho* butterfly structures is the finite element method (FEM). In comparison to standardized FDTD, FEM analysis for *Morpho* applications is new; however, it is based on a comparable simulation operation. The FEM simulations solve Maxwell's equations using a commercial software package (e.g., Comsol Multiphysics), which is less time consuming as a result of its flexible triangular mesh while maintaining accuracy. Using the FEM, the effects of different structural properties such as alternating lamella, a "Christmas tree"-like shape, and offsets between neighboring ridges, and their influence on wide angle deflection

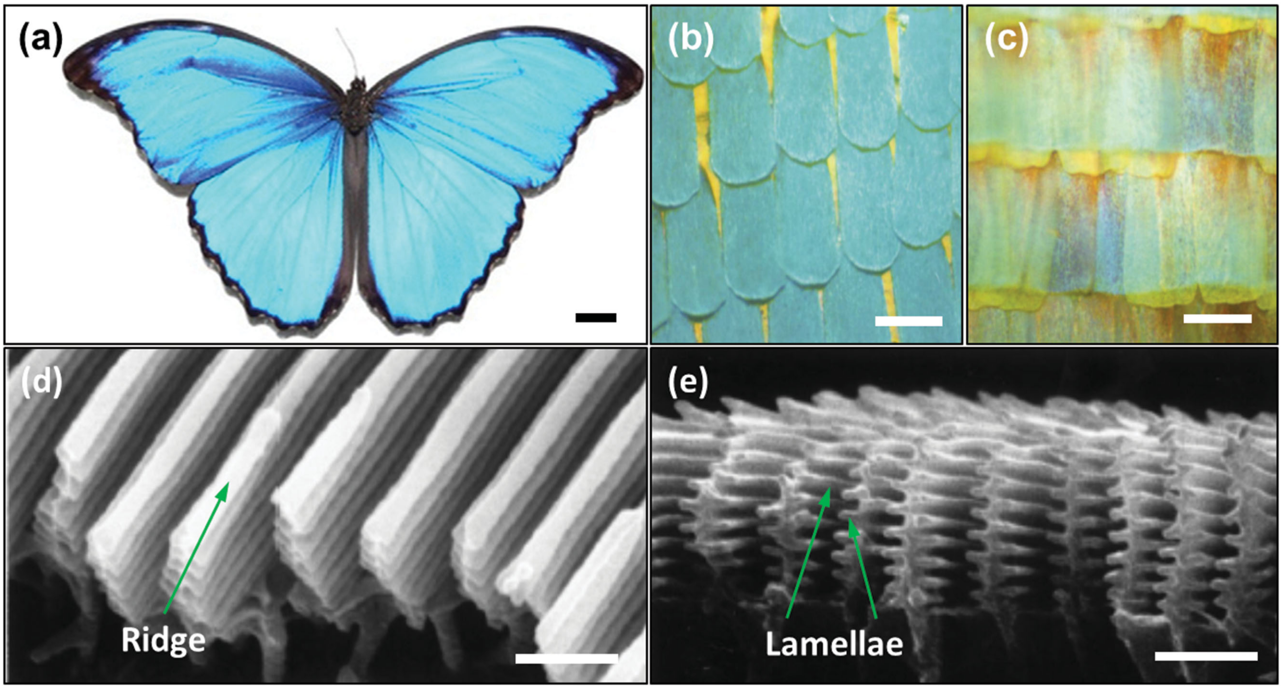

Figure 1. Nanostructure of the *Morpho* butterfly. a) A photograph of the *Morpho didius* butterfly showing blue iridescence. Scale bar = 1 cm, Reproduced with permission.[8] Copyright 2011, Elsevier. b) A magnified image of an *M. rhetanor* wing showing the ordered arrangement of its single layer of ground scales. Scale bar = 100 µm. c) A magnified image of an *M. didius* wing illustrating the two distinct types of scales, with the glass scales overlying the ground scales, scale bar = 100 µm. Panels (b) and (c) reproduced with permission.[9] Copyright 1999, The Royal Society. d) Scanning electron microscope (SEM) images of an oblique view of the male butterfly *M. didius*. Scale bar = 1 µm. e) A cross-section of a ground scale of the male butterfly *Morpho didius*. Scale bar = 1 µm. Panels (d) and (e) reproduced with permission.[10] Copyright 2012, The Royal Society.

were investigated.[15] Additionally, *Morpho* scale architectures can also be simulated by the rigorous coupled-wave analysis (RCWA).[8,24] It utilizes the software module DiffractMOD that implements various algorithms, including a fast converging of Maxwell's equations. **Table 1** shows the list of analytical techniques associated with *Morpho* butterfly models.

3. Replication of *Morpho* Scale Nanostructures

Through advances in nanotechnology, several attempts have been made to mimic the photonic structure and the iridescent features of the *Morpho* butterfly scales.[15,27] Biotemplating (or biomineralization) has been utilized to deposit a compatible oxide onto an organic *Morpho* wing template to preserve the exact features of the structure. Lithography was also used for fabricating *Morpho* nanostructures, focusing on the reproduction of the bright blue color instead of replicating the exact structure. Recently, dual-beam laser interference lithography (LIL) was utilized for *Morpho* replication.

3.1. Deposition-Directed Replication of *Morpho* Butterfly Scales

Biotemplating wing scales is a commonly used method to produce accurate replicas. A scale structure was replicated using atomic layer deposition (ALD) by coating a butterfly wing sample with an alumina (Al_2O_3) layer at 100 °C.[27] The thickness of each layer was controlled by varying the cycle of deposition. After the cycles were completed, the original butterfly wing was burned out in the presence of oxygen by annealing the sample at 800 °C for 3 h to produce a wing shell. The sample was further crystallized into a robust structure. This method preserved the complex structure of the *Morpho* wing, due to the uniformity of the Al_2O_3 coating (**Figure 3**a). In complex nanostructures, achieving uniform and conformal features by ALD is limited by the degree of saturation and surface diffusion behavior.[28,29] The ALD method is low cost and is reproducible while providing accurate control over the nanostructure geometry. However, obtaining large numbers of natural wing samples is obviously a challenge for the mass production of butterfly structures.

Another replication of a *Morpho* nanostructure through ALD consisted of a "Christmas tree"-resembling structure.[29] This method was similar to the previously reported approach except that the deposition temperature of Al_2O_3 was 80 °C. Additionally, silica replication was reported, which involved copying the wing of the *Morpho rhetanor*. The fabrication was performed through physical vapor deposition (PVD) under pretested conditions that preserved the multilayers of the butterfly ridges and scales (Figure 3a).[30] The same study also contained a titania-based replication of the *Morpho menelaus* by chemical solution deposition (CSD; see Figure 3b). The fabrication involved a sol–gel process for replicating the lepidopteran wings.[18] Other procedures combined with this technique were solution evaporation and dip coating.[30] Although the conditions of this method

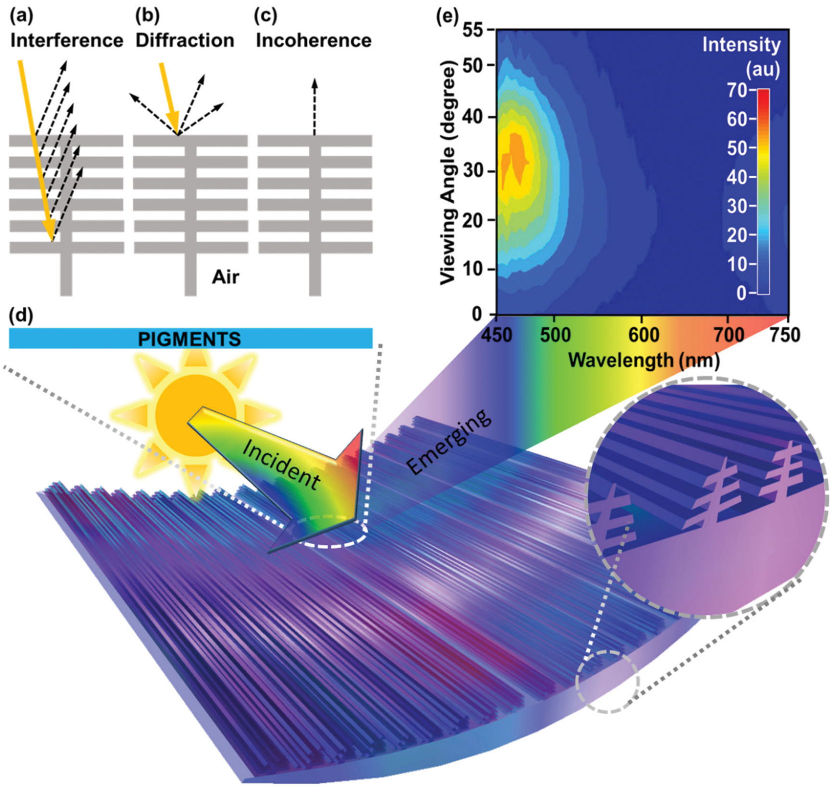

Figure 2. Principles of the blue coloration in the *Morpho* butterfly. a) Multilayer interference, b) diffraction, and c) incoherence. d) Pigment layer. e) Angle-resolved measurements of the back scattered light from *M. rhetenor*. Reproduced with permission.[16] Copyright 2014, Nature Publishing Group.

were more desirable than those for PVD (ambient pressure and room temperature), the replicas produced were fragile due to cracking. Recently, PVD was utilized to selectively modify the lamella layer of *Morpho sulkowskyi*.[32] The edges of lamella were exposed to an incoming flux of gold to form a layer of 50 nm. The gold-modified wing structures had IR absorbance that allowed tuning of the lamella nanostructure.

Experimentation with sol–gels has enabled the formation of an intricate, continuous, and conformal nanocrystalline *Morpho* scale structures. A foundation of titanium dioxide was used to produce distortion-free 3D nanostructures. The basis of this method relied on the chitin content found in the wing scales, providing the hydroxyl groups required to initiate the sol–gel process.[31] Thin layers of oxide were coated onto the *Morpho* wing through layer-by-layer (LBL) deposition using a computer-controlled sol–gel process (Figure 3d).[18] The wings were then annealed at 900 °C. Finally, conversion of the structure into rutile titania replicas was executed by using a surface sol–gel process with tin(IV) isopropoxide as a rutile-promoting dopant.[31] This method has the same limitation as the ALD proposition, that is, the fabrication requires an organic (or synthetic) template. Using a synthetic template requires an additional step, which is time consuming and costly. However, there are many benefits of a sol–gel-controlled process, such as facile shape control, mild reaction conditions, and compatibility with a wide variety of chemicals.[33] Additionally, the structure of the material can be controlled down to a sub-micrometer level from the earliest stage of processing.

Focused ion beam-assisted chemical vapor deposition (FIB-CVD) was also utilized for replications (Figure 3e). Initially a 3D mold was fabricated by producing 3D computer-aided design (CAD) data, which was converted to a scanning signal, as an FIB scanning apparatus to form the final mold.[13] The FIB system formed the *Morpho* quasi-structure by deposition of $C_{14}H_{10}$ (phenanthrene), which was selected as the source due to its high deposition rate as compared to previously tested specimens of C_8H_8 (styrene) and $C_{16}H_{10}$ (pyrene) (Figure 3d). The drawbacks of this method are its high cost and limited scalability, despite being able to produce accurate *Morpho* nanostructures of the same shape and size while maintaining comparable optical characteristics of the original wing scale.[18]

Table 1. Analytical and numerical analysis methods in *Morpho* butterfly models.

	Method	Description	Features and Limitations	Ref.
Analytical	Multilayer theory	Based on multilayer grating equations	Allows fast calculation of transmission and reflection spectra	[5,9]
	Lamellar grating electromagnetic theory	Converting reflection coefficients of any structure into colours	Allows obtaining color maps to have a global insight of reflection properties of the modelled structure. The tilted ridges are not taken into account.	[20,25]
Numerical	FDTD	Quasi-periodic arrangement of tree-like structures	Computes scattered field intensities due to infinite cylinders. The method is slower compared to others.	[4,21–23,26]
	FEM	Solves Maxwell's equation using COMSOL Multiphysics and related softwares	Utilizes flexible triangle-shaped mesh with high accuracy and speed.	[15]
	RCWA	Models constructed by DiffractMOD, which is a general design tool for optically diffractive structures	Implements algorithms including a fast converging formulation of Maxwell equations and a numerical stabilization scheme	[8,24]

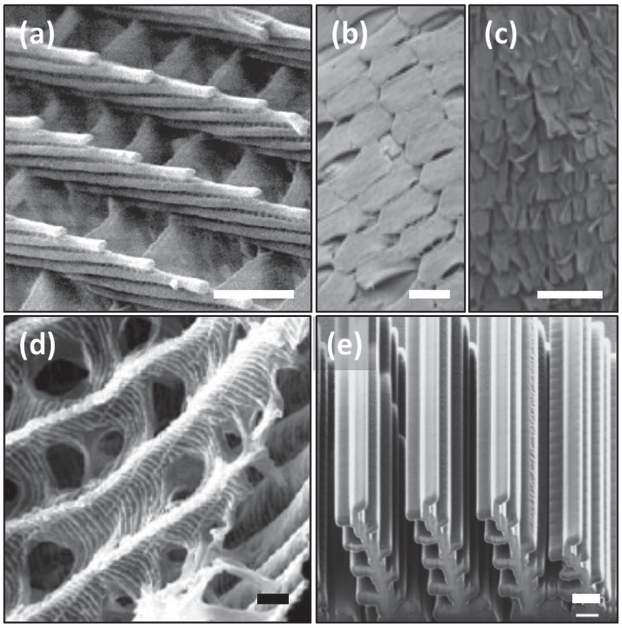

Figure 3. *Morpho* replication. a) SEM images of an alumina-templated scale, where the replica exhibits fine structures, scale bar = 1 µm. Reproduced with permission.[27] Copyright 2006, American Chemical Society. b) SEM image of *M. rhetenor* scales after physical deposition of SiO_2, scale bar = 100 µm. c) SEM image of *M. menelaus* scales after sol–gel deposition of TiO_2. Scale bar = 100 µm. Panels (b) and (c) reproduced with permission.[30] Copyright 2014, Elsevier. d) SEM image of scales exposed to 40 surface sol–gel deposition cycles involving a mixed 2-propanol solution of titanium(IV) isopropoxide and Sn(IV) isopropoxide, scale bar = 1 µm. Reproduced with permission.[31] Copyright 2008, John Wiley & Sons, Inc. e) Inclined-view SEM image of *Morpho* butterfly scale quasi-structure fabricated by FIB-CVD, scale bar = 1 µm. Reproduced with permission.[13] Copyright 2005, Japan Society of Applied Physics.

3.2. Lithographic Replication of *Morpho* Butterfly Scales

The earliest replications through lithography involved the fabrication of multilayer structures to mimic the *Morpho* scales by depositing layers of SiO_2 and TiO_2 onto a nanopatterned surface (**Figure 4**a). The initial nanopattern was engraved onto a quartz substrate, by a combination of electron beam lithography (EBL) and dry etching, which is a crucial stage in the process to achieve the accurate dimensions of the pattern. This method does not produce a structure emulating the exact features of the *Morpho* nanostructure, instead it focuses on reproducing the optical characteristics of the blue iridescence by controlling the size of the lattice spacing and width engraved onto the substrate. Finally, seven pairs of SiO_2 and TiO_2 layers (40 nm thick) were LBL coated onto the fabricated nanopattern using electron beam deposition. The thickness of oxides could be controlled more accurately over other materials during deposition which influenced their usage in this process. Although EBL can produce nanoscale patterns with high resolution, the fabrication is time consuming, and high cost.

Nanocasting lithography (NCL) was also utilized to produce a multilayer structure by modifying the original lithography method. A master substrate featuring the initial ridges was produced by conventional nanoimprint lithography (NIL). This master substrate acted as a template to directly nanopattern UV curable resin using the NCL (**Figure 5**a–d).[35] To form the multilayer structures within the ridges, the same deposition technique was used (Figure 5e). This method was advantageous as costs are significantly reduced since it only required a conventional mask aligner and a spin coater. These approaches allowed mass production by eliminating two high-cost and multistep processes: EBL and dry etching.[36]

The accuracy of replica nanostructures was further developed by having an homogeneous and scalable template mold. This process featured a fs laser to form the initial mold containing ridges (replacing NIL), combined with electroforming (replacing EBL) to create irregular multilayers within the structure.[37] This method provided a faster production time while keeping the structures anisotropic and random. A soft lithography technique was also investigated to create a multilayered structure of the upper *Morpho* scales.[34] The fabrication consisted of a four step process that transformed polydimethylsiloxane (PDMS) into the proposed nanostructure (Figure 4c). LIL was also explored to replicate the photonic structure of the *Morpho* butterfly scale.[38] Initially, a glass substrate was spin coated with a photoresist, which was then exposed to a two laser beams (**Figure 6**). The substrate was coated with a reflective coating to induce a vertical secondary interference. The beams were kept homogenous by the use of pinholes to eliminate high-frequency distortions and a quartz plate moderated transmitted power through one beam path. Figure 6 also shows the resulting “Christmas tree” nanostructure.

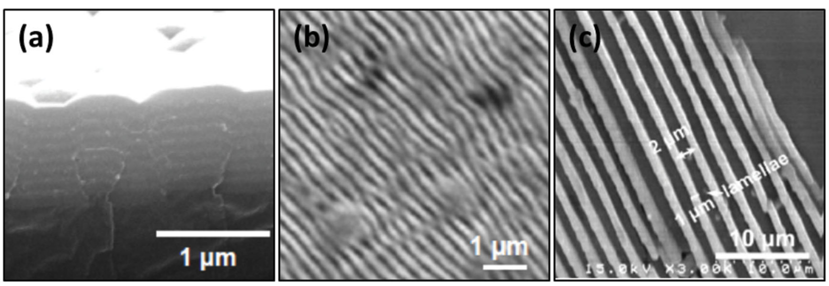

Figure 4. Lithographic replication of butterfly scales. A) Image of discrete multilayers formed on the nanopatterned plate by nanocasting lithography. Reproduced with permission. Copyright 2009, Society of Photo Optical Instrumentation Engineers. b) SEM image of the ripple (nanogroove) pattern made by fs-laser fabrication (after electroforming on Ni plate). Pitch = 300 nm. Reproduced with permission. Copyright 2012, Society of Photo Optical Instrumentation Engineers. c) Characteristics of a butterfly wing: ridge-like structures on replicated scale surface via soft lithography. Reproduced with permission.[34] Copyright 2010, Elsevier.

Titania was also utilized to form a hierarchical structure featuring mesopores to improve light absorption. The method involved two pretreated *Morpho* wings, which were ultra-sonicated at room temperature with a high intensity probe.[39] Finally, calcination was performed, and wing remnants were removed to form titania-based structures.[39] **Table 2** shows the fabrication methods for replicating *Morpho* scales.

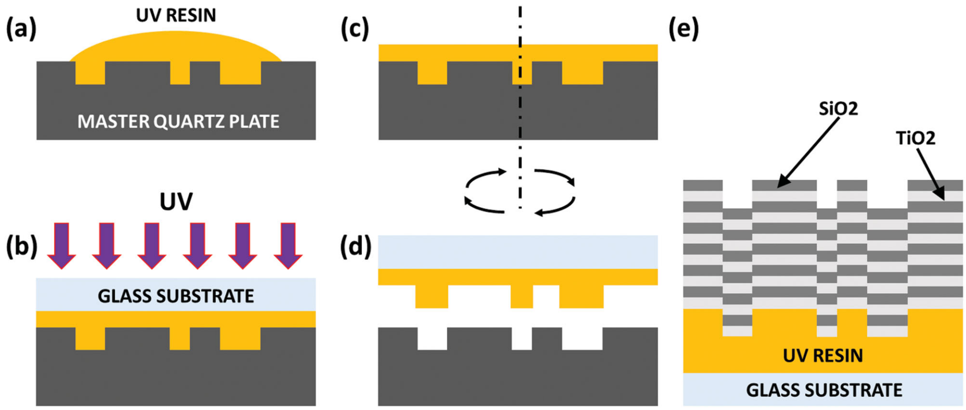

Figure 5. Reproduction of the *Morpho* blue structures via NCL. The master plate is replicated by NCL using UV curable resin, and the SiO_2 and TiO_2 layers are deposited on the cured resin pattern. a) Deposition of UV resin on the substrate. b) Spin coating. c) A glass slide is placed on top and UV is exposed to the resin. d) Release of the master plate. e) Deposition of multilayered thin films on the replicated resin plate.

4. Applications of *Morpho* Butterfly Scale Replicas

The *Morpho* butterfly demonstrates unique optical properties that can be applied to the developments in photonic devices. General Electric Global Research Center (GEGRC) has studied the scales of the *Morpho sulkowskyi* for gas sensing. The reflectance spectra of the structure within the scales vary with exposure to different vapors. A group of organic vapors: methanol, ethanol, and dichloroethylene were distinguished by analyzing reflectance as a function of time.[25,40] By experimenting with different concentrations of each vapor, highly sensitive properties of the scales were discovered. This behavior was attributed to the ridge-lamella structure within the scales. Existing nanofabricated structures may identify closely related vapors, and thus require layers of chemicals to enhance selectivity. Another Morpho butterfly-inspired sensor was utilized to detect different vapors.[41] After the nanostructures were fabricated by e-beam lithography, they were coated with monolayers of a fluorine-terminated silane. To test the selectivity, they were exposed to benzene, methyl ethyl ketone, acetonitrile, methanol and water. The sensors selectively detected separate vapors in pristine conditions and quantified these vapors in mixtures in the presence of moisture background.

Further development by GEGRC has led to the production of a biomimetic chitin-based thermal sensor inspired by the *Morpho* nanostructure. The sensor was designed to detect mid-wave infrared light, since chitin has infrared absorption properties, and the optical properties of the sensor were similar to the vapor sensor. The *Morpho* wing structure was temperature sensitive: when the surrounding temperature increased, the hierarchical structure was thermally expanded. This increased the spacing between ridges, resulting in a thermally induced reduction in the effective refractive index of the structure.[42] Hence, the shift in the intensity of the diffracted light at a fixed wavelength was converted into a measurable temperature change. Additionally, the wing scales were doped with single-walled carbon nanotubes (SWCNTs) to enhance the structure's infrared absorption properties.[42] Not only does this technique increased the sensitivity of the device, it improved thermal conductivity and thermal conversion of NIR photons. The improved thermal coupling between the chitin wing structure and the SWCNTs enabled the scales to efficiently convert incident radiation into visible iridescence changes, which has application in thermal imaging devices.

5. Future Directions

The nanoarchitecture of replicated *Morpho* butterfly scales can be potentially functionalized to be specific to a wide range of analytes. Recently, multilayer diffraction grating constructed via silver halide and laser ablation holography in hydrogel matrices enabled analyte-specific recognition.[43] Such multilayer structures have been functionalized with acrylic acid, porphyrin derivatives, 8-hydroxyquinoline, and boronic acid to be sensitive to pH, metal ions, and carbohydrates.[44] The applications of these materials to *Morpho*-inspired nanoarchitectures can expand the existing selectivity and sensing capabilities for application in medical diagnostics, environmental monitoring, and food testing. Such devices may also be patterned using laser writing to form optical devices such as lenses and diffusers, or printed on flexible substrates.[45] *Morpho* nanarchitectures may also be combined with emerging materials such as graphene and carbon nanotubes to introduce new functionalities such as high mechanical strength, electrical conductivity, and transparency.[46] These devices may be multiplexed by using microfluidic devices, integrated into contact lenses, or quantified by smartphone cameras.[47] Additionally, *Morpho* inspired solar cells

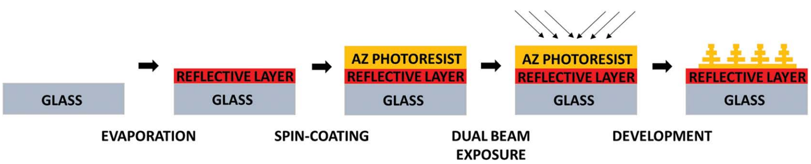

Figure 6. Fabrication process of horizontal structures by dual beam LIL. A photoresist is spin coated on a clean glass substrate and exposed by two interfering laser beams. The development of the photoresist results in a "Christmas tree"-like photonic structure on the glass substrate.

Table 2. Nanofabrication methods of *Morpho* butterfly scales.

Replication/Method	Feature	Dimension	Sample Size	Ref.
ALD	Inversed 2D biotemplated structure	Each alumina layer 41 nm thick	Each repeating unit was 50 × 60 nm	[27]
PVD	Inversed 2D biotemplated structure	Deposited silica layer 2 µm	Substrate distance 4 cm	[30]
CSD	Inversed 2D biotemplated structure	Deposited titania layer 2 µm	Substrate distance 4 cm	[30]
LBL deposition combined with sol–gel processes	3D nanocrystalline structure	Each oxide coating ≈ 60 nm thick and average crystallite size ≈ 15 nm	1.5 × 1.5 cm	[31]
FBI-CVD	3D quasi-structure	2.60 µm in height, 0.26 µm in width, 20 µm in length and had a 0.23 mm grating pitch	N/A	[13]
ALD	"Christmas tree" structure	Approximately the same size as the Morpho scales. The structures had ≈ 0.8 µm separation and ≈ 1.8 µm height.	N/A	[29]
EBL	Multilayer structure	Rectangular units of 3000 nm × 2000 nm and depth of pattern at 110 nm	N/A	[35]
NCL	Multilayer structure	900 nm high	N/A	[35]
fs-laser patterning, electroforming and deposition	Irregular multilayer structure	N/A	15 × 15 mm and 85 × 85 mm	[37]
LIL	"Christmas tree" 3D structure	Layer thickness ≈ 40 nm and air gap ≈ 40 nm	N/A	[38]
Soft lithography	Multilayer 3D structure	Ridge scale sizes varying between 1.5–2.0 µm. Lamella of width ≈1 µm with neighbors separated by an air gap ≈2 µm	N/A	[34]
Ultra-sonication	Multilayer structures featuring mesopores	Inter-lamella spacing of 1.05–1.01 µm and grain sizes of 14.3–11.1 nm	N/A	[39]

has been proposed, but they have not been experimentally demonstrated yet.[2,48]

The *Morpho* butterfly wings contain rare 3D geometrical structures, which are effectively responsible for their bright blue irradiance colors. We have presented an overview of computational methods which have been used to optimize the optical properties and effects displayed by *Morpho* nanostructures. A range of nanofabrication methods that accurately produce replicas of these 3D nanostructures has been described. We anticipate that the replicas of *Morpho* butterfly wings will find myriad applications in highly sensitive optical sensing, imaging, and efficient photovoltaics.

Acknowledgements

H. Butt, A. K. Yetisen, and D. Mistry wrote the article. D. Mistry, S. A. Khan, M. U. Hassan, and S. H. Yun edited the manuscript. H. Butt and A. K. Yetisen contributed equally to this work. The authors declare no competing financial interests. H. Butt thanks the Leverhulme Trust for the research funding.

Received: November 6, 2015
Revised: December 17, 2015
Published online: January 11, 2016

[1] a) P. Vukusic, J. R. Sambles, *Nature* **2003**, *424*, 852; b) M. Srinivasarao, *Chem. Rev.* **1999**, *99*, 1935.
[2] S. Lou, X. Guo, T. Fan, D. Zhang, *Energy Environ. Sci.* **2012**, *5*, 9195.
[3] K. Watanabe, T. Hoshino, K. Kanda, Y. Haruyama, T. Kaito, S. Matsui, *J. Vacuum Sci. Technol. B* **2005**, *23*, 570.
[4] S. Banerjee, J. B. Cole, T. Yatagai, *Micron* **2007**, *38*, 97.
[5] S. Kinoshita, S. Yoshioka, Y. Fujii, N. Okamoto, *FORMA* **2002**, *17*, 103.
[6] S. Kinoshita, S. Yoshioka, *ChemPhysChem* **2005**, *6*, 1442.
[7] T. F. Anderson, A. G. Richards, *J. Appl. Phys.* **1942**, *13*, 748.
[8] X. Yang, Z. Peng, H. Zuo, T. Shi, G. Liao, *Sens. Actuat. A* **2011**, *167*, 367.
[9] P. Vukusic, J. R. Sambles, C. R. Lawrence, R. J. Wootton, *Proc. R. Soc. B*, **1999**, *266*, 1427.
[10] S. Kinoshita, S. Yoshioka, K. Kawagoe, *Proc. R. Soc. B* **2002**, *269*, 1417.
[11] S. Yoshioka, S. Kinoshita, *Proc. R. Soc. B* **2004**, *271*, 581.
[12] G. S. Smith, *Am. J. Phys.* **2009**, 77.
[13] K. Watanabe, T. Hoshino, K. Kanda, Y. Haruyama, S. Matsui, *Jap. J. Appl. Phys.* **2005**, *44*, L48.
[14] B. Song, S. C. Eom, J. H. Shin, *Opt. Express* **2014**, *22*, 19386.
[15] R. H. Siddique, S. Diewald, J. Leuthold, H. Hölscher, *Opt. Express* **2013**, *21*, 14351.
[16] W. Wang, W. Zhang, X. Fang, Y. Huang, Q. Liu, J. Gu, D. Zhang, *Sci. Rep.* **2014**, 4.
[17] S. Kinoshita, S. Yoshioka, K. Kawagoe, *Proc. R. Soc. B* **2002**, *269*, 1417.
[18] D. Zhang, W. Zhang, J. Gu, T. Fan, Q. Liu, H. Su, S. Zhu, *Prog. Mater. Sci.* **2015**, *68*, 67.
[19] K. Yu, T. Fan, S. Lou, D. Zhang, *Prog. Mater. Sci.* **2013**, *58*, 825.
[20] B. Gralak, G. Tayeb, S. Enoch, *Opt. Express* **2001**, *9*, 567.
[21] S. Banerjee, Z. Dong, *Opt. Rev.* **2007**, *14*, 359.
[22] R. T. Lee, G. S. Smith, *Appl. Opt.* **2009**, *48*, 4177.
[23] M. A. Steindorfer, V. Schmidt, M. Belegratis, B. Stadlober, J. R. Krenn, *Opt. Express* **2012**, *20*, 21485.
[24] T. Jiang, Z. Peng, W. Wu, T. Shi, G. Liao, *Sens. Actuat. A* **2014**, *213*, 63.

[25] R. A. Potyrailo, H. Ghiradella, A. Vertiatchikh, K. Dovidenko, J. R. Cournoyer, E. Olson, *Nat. Photon.* **2007**, *1*, 123.
[26] D. Zhu, S. Kinoshita, D. Cai, J. B. Cole, *Phys. Rev. E* **2009**, *80*, 051924.
[27] Huang, WangWang, Z. L. Wang, *Nano Lett.* **2006**, *6*, 2325.
[28] H. Kim, H.-B.-R. Lee, W. J. Maeng, *Thin Solid Films* **2009**, *517*, 2563.
[29] F. Liu, Y. Liu, L. Huang, X. Hu, B. Dong, W. Shi, Y. Xie, X. Ye, *Optics Commun.* **2011**, *284*, 2376.
[30] M. Thomé, L. Nicole, S. Berthier, *Mater. Today* **2014**, *1S*, 221.
[31] M. R. Weatherspoon, Y. Cai, M. Crne, M. Srinivasarao, K. H. Sandhage, *Angew. Chem.* **2008**, *120*, 8039.
[32] F. Zhang, Q. Shen, X. Shi, S. Li, W. Wang, Z. Luo, G. He, P. Zhang, P. Tao, C. Song, *Adv. Mater.* **2015**, *27*, 1077.
[33] W. Zhang, J. Gu, Q. Liu, H. Su, T. Fan, D. Zhang, *Phys. Chem. Chem. Phys.* **2014**, *16*, 19767.
[34] S.-H. Kang, T.-Y. Tai, T.-H. Fang, *Curr. Appl. Phys.* **2010**, *10*, 625.
[35] A. Saito, M. Nakajima, Y. Miyamura, K. Sogo, Y. Ishikawa, Y. Hirai, *Proc. SPIE 6327, Nanoengineering: Fabrication, Properties, Optics, and Devices II*, San Diego, California, USA, September, **2006**
[36] A. Saito, Y. Miyamura, Y. Ishikawa, J. Murase, M. Akai-Kasaya, Y. Kuwahara, *Proc. SPIE 7205, Advanced Fabrication Technologies for Micro/Nano Optics and Photonics II,* **2009**, *7205*, 720506.
[37] A. Saito, J. Murase, M. Yonezawa, H. Watanabe, T. Shibuya, M. Sasaki, T. Ninomiya, S. Noguchi, M. Akai-kasaya, Y. Kuwahara, *Proc. SPIE 8339, Bioinspiration, Biomimetics, and Bioreplication* **2012**, *8339*, 83390C.
[38] R. H. Siddique, A. Faisal, R. Hünig, C. Bartels, I. Wacker, U. Lemmer, H. Hölscher, *Proc. SPIE 9187, The Nature of Light: Light in Nature V* **2014**, *9187*, 91870E.
[39] X. Liu, S. Zhu, D. Zhang, Z. Chen, *Mater. Lett.* **2010**, *64*, 2745.
[40] R. Bogue, *Sens. Rev.* **2009**, *29*, 107.
[41] R. A. Potyrailo, R. K. Bonam, J. G. Hartley, T. A. Starkey, P. Vukusic, M. Vasudev, T. Bunning, R. R. Naik, Z. Tang, M. A. Palacios, *Nat. Commun.* **2015**, 6.
[42] A. D. Pris, Y. Utturkar, C. Surman, W. G. Morris, A. Vert, S. Zalyubovskiy, T. Deng, H. T. Ghiradella, R. A. Potyrailo, *Nat. Photon.* **2012**, *6*, 195.
[43] a) C. P. Tsangarides, A. K. Yetisen, F. da Cruz Vasconcellos, Y. Montelongo, M. M. Qasim, T. D. Wilkinson, C. R. Lowe, H. Butt, *RSC Adv.* **2014**, *4*, 10454; b) A. K. Yetisen, Y. Montelongo, N. M. Farandos, I. Naydenova, C. R. Lowe, S. H. Yun, *Appl. Phys. Lett.* **2014**, *105*, 261106; c) A. K. Yetisen, H. Butt, L. R. Volpatti, I. Pavlichenko, M. Humar, S. J. Kwok, H. Koo, K. S. Kim, I. Naydenova, A. Khademhosseini, S. K. Hahn, S. H. Yun, *R. Biotechnol. Adv*. **2015**, DOI: 10.1016/j.biotechadv.2015.10.005.
[44] a) A. K. Yetisen, H. Butt, F. da Cruz Vasconcellos, Y. Montelongo, C. A. Davidson, J. Blyth, L. Chan, J. B. Carmody, S. Vignolini, U. Steiner, *Adv. Optical Mater.* **2014**, *2*, 250; b) A. Yetisen, M. Qasim, S. Nosheen, T. Wilkinson, C. Lowe, *J. Mater. Chem. C* **2014**, *2*, 3569; c) A. K. Yetisen, Y. Montelongo, M. M. Qasim, H. Butt, T. D. Wilkinson, M. J. Monteiro, S. H. Yun, *Analyt. Chem.* **2015**, *87*, 5101; d) A. K. Yetisen, Y. Montelongo, F. da Cruz Vasconcellos, J. L. Martinez-Hurtado, S. Neupane, H. Butt, M. M. Qasim, J. Blyth, K. Burling, J. B. Carmody, M. Evans, T. D. Wilkinson, L. T. Kubota, M. J. Monteiro, C. R. Lowe, *Nano Lett.* **2014**, *14*, 3587; e) A. K. Yetisen, I. Naydenova, F. da Cruz Vasconcellos, J. Blyth, C. R. Lowe, *Chem. Rev.* **2014**, *114*, 10654.
[45] a) Q. Zhao, A. K. Yetisen, A. Sabouri, S. H. Yun, H. Butt, *ACS Nano* **2015**, *9*, 9062; b) Q. Zhao, A. K. Yetisen, C. J. Anthony, W. R. Fowler, S. H. Yun, H. Butt, *Appl. Phys. Lett.* **2015**, *107*, 041115; c) X.-T. Kong, A. A. Khan, P. R. Kidambi, S. Deng, A. K. Yetisen, B. Dlubak, P. Hiralal, Y. Montelongo, J. Bowen, S. Xavier, K. Jiang, G. A. J. Amaratunga, S. Hofmann, T. D. Wilkinson, Q. Dai, H. Butt, *ACS Photonics* **2015**, *2*, 200; d) F. d. C. Vasconcellos, A. K. Yetisen, Y. Montelongo, H. Butt, A. Grigore, C. A. B. Davidson, J. Blyth, M. J. Monteiro, T. D. Wilkinson, C. R. Lowe, *ACS Photonics* **2014**, *1*, 489.
[46] a) H. Butt, A. K. Yetisen, R. Ahmed, S. H. Yun, Q. Dai, *Appl. Phys. Lett.* **2015**, *106*, 121108; b) S. Deng, A. K. Yetisen, K. Jiang, H. Butt, *RSC Adv.* **2014**, *4*, 30050; c) X.-T. Kong, H. Butt, A. K. Yetisen, C. Kangwanwatana, Y. Montelongo, S. Deng, F. da Cruz Vasconcellos, M. M. Qasim, T. D. Wilkinson, Q. Dai, *Appl. Phys. Lett.* **2014**, *105*, 053108.
[47] a) L. R. Volpatti, A. K. Yetisen, *Trends Biotechnol.* **2014**, *32*, 347; b) N. M. Farandos, A. K. Yetisen, M. J. Monteiro, C. R. Lowe, S. H. Yun, *Adv. Healthc. Mater.* **2015**, *4*, 792; b) A. K. Yetisen, J. Martinez-Hurtado, A. Garcia-Melendrez, F. da Cruz Vasconcellos, C. R. Lowe, *Sens. Actuat. B* **2014**, *196*, 156; c) A. K. Yetisen, J. L. Martinez-Hurtado, F. da Cruz Vasconcellos, M. C. Simsekler, M. S. Akram, C. R. Lowe, *Lab Chip* **2014**, *14*, 833; d) A. K. Yetisen, M. S. Akram, C. R. Lowe, *Lab Chip* **2013**, *13*, 2210.
[48] B. D. Heilman, l. N. Miaoulis, *Appl. Optics* **1994**, *33*, 6642.